On management strategies depending on the number of infected in order to stop a SEIRS epidemic: case of the Covid-19 pandemic

Pierre Auger, Ali Moussaoui, Tri Nguyen Huu

On management strategies depending on the number of infected in order to stop a SEIRS epidemic: case of the Covid-19 pandemic

Pierre Auger[b], Ali Moussaoui[a], Tri Nguyen Huu[b,c]

[a] *Laboratoire d'Analyse Non linéaire et Mathématiques Appliquées, Université de Tlemcen, Faculté des Sciences, Département de Mathématiques, Algérie*
[b] *Sorbonne Université, IRD, UMMISCO, F-93143, Bondy, France*
[c] *IXXI, ENS Lyon, Lyon, France*

Abstract

The aim of this work is to evaluate the efficiency, benefits and costs of different strategies for managing an epidemic described by a classic SEIRS model. Non-Pharmaceutical Interventions are taken by health authorities in order to remove a certain proportion of people from the chain of contamination, such as quarantine, partial lockdown as well as teleworking. We further assume that the intensity of protective measures is infected dependent. Depending on the choice of the infected dependent control function, we show that it is possible to create new endemic equilibria or change the stability of the disease-free equilibrium. We present the mathematical analysis, existence and stability properties of equilibria. We present several management strategies grouped into four main classes. Appart from constant level strategies, we particularly study the effects of management strategies that allow the number of cases to be stabilized at a target low endemic level or else to generate an "Allee" effect that allows to extinguish the epidemic below some threshold. We compare the different strategies and discuss the opportunity to apply the method in the case of the SARS-CoV-2 epidemic.

Keywords: SEIRS, infectious dependent management of an epidemic, target endemic level, Allee effect, SARS-Cov-2.

1. Introduction

The onset of the Covid-19 epidemic was brutal with very high peaks of contamination leading to the saturation of intensive care units. In the United States, the occupancy rate of intensive care beds reached over 60% in the most populous states and large cities [7]. In France, the number of beds able to accommodate severely ill patients requiring intensive care in hospitals is limited to around 5,000 beds and the number of respirators available seemed also insufficient in view of the foreseeable arrival of seriously ill patients. As a result, several governments in the world have decided to put in place more or less strict Non Pharmaceutical Interventions (NPI) such as lockdown, social distancing or teleworking in order to limit the number of cases and keep hospital admissions of seriously ill patients below the hospital capacity threshold. This policy has been adopted by many countries

and has worked with some success. Hospitals were under very strong pressure but were able throughout the epidemic wave to treat the patients requiring intensive care.
However, lockdown has had disastrous consequences for the economy, generating waves of unemployment, causing considerable budget deficits for the states, with very serious difficulties for those in need. Some countries have chosen to set up a partial lockdown while maintaining activity or have opted to end the lockdown early enough to limit the disastrous consequences for their economy, especially in Northern Europe. Many countries remain extremely cautious in this area, fearing the occurrence of successive epidemic waves after lockdown. The question of the end of lockdown is therefore crucial and it is important to develop scientific methods allowing to control this phase by limiting the damage. Much work has been devoted to modeling the covid epidemic: [1, 12, 5] in China, [17, 23, 14] in Japan, [18, 19, 4] in Algeria. We present here a theoretical approach aiming at evaluating the effects of some NPI against the Covid-19 epidemic and their ability to fulfill some requirements such as keeping the number of cases at a level low enough to be managed by hospitals, or maintaining a lockdown at a level low enough to avoid consequences that are too damaging to the economy. We cite [13] in which the authors studied the effects of different quarantine and protection measures on the dynamics of the epidemic with a mathematical model, and [25] for Canada.

The article is made up of several sections. After an introductory part, section 2 presents the SEIRS epidemic model with infected dependent control, the mathematical analysis of the epidemic model, existence of endemic equilibria and stability properties. In section 3, we compare several infection-dependent NPI strategies. Among these, we present a constant level strategy, a strategy to avoid a large-scale epidemic peak and to stabilize the epidemic at an endemic level low enough to avoid congestion in hospitals and two strategies that allow to generate an Allee effect which permits to provoke the extinction of the epidemic below some endemic threshold. Section 4 presents a discussion of the results with a comparison of the different strategies showing the advantages, limitations and costs of each one. We discuss the application of the method to the SARS-CoV-2 epidemic.

2. SEIRS model with NPI depending on the number of infected people

We consider an epidemic focus, such as a city where the epidemic has just started. It is normally necessary to take into account the urban mobility of individuals in the dynamics of the epidemic. We cite the work [16], in which aged structured individuals are supposed to move between their place of residence, workplaces, universities, schools, public places, shopping centers and more places, [26] and [21]. In our model, [4], we also took into account the daily movements of people between their home and the various places where they are required to move and where they are more or less protected from contact with infectious persons as well as confinement and protection by masks following the work by [11].

2.1. Description of the SEIRS model

One way to derive the following SEIRS model would be to consider the version of the baseline confinement model in [4] and to assume that the proportion of people confined

depends on the number of people infected, $v(I)$. However, we will now give more details on the constituent elements of our model. We consider a classical SEIRS model in which individuals can switch between a normal state and a state in which they are removed from the dynamics because of isolation or social distancing. We consider that NPI such as self isolation or lockdown result in a proportion v of the population being in the state of isolation. We emphasize on the fact that maintaining a proportion v of the population in state of isolation does not mean that the population is separated in two groups (one group with individuals that stay in normal state, and the other with individuals that stay isolated), but that individuals can change state as long as this proportion remains constant. A NPI that imposes two days of teleworking per labour week (five days) would result in a proportion $v = 40\%$ of isolated people working from home every day. However people may be in a different state every day. In the following sections, v will refer to a more general definition of NPI intensity that will not only apply to lockdown or teleworking but also to social distancing or mask wearing, by assuming that any measure is equivalent to a percentage of time spent in isolation.

Infected individuals follow the natural process of the disease corresponding to a classical SEIRS model, i.e exposed individuals can become infected after an incubation time $\frac{1}{k}$, infected individuals can recover or are removed after a time $\frac{1}{\alpha}$, and they lose their immunity after a time $\frac{1}{\gamma}$. The number of newly infected individuals per unit of time for the population in a classical SEIRS model is given by the expression $\beta\frac{SI}{N}$, where β is the transmission rate of the disease for one infectious individual in a population with only susceptible individuals. Since only infected individuals that are not isolated can contaminate others, and since only susceptible individuals that are not isolated can be contaminated, this expression must be replaced by $\beta\frac{(1-v)S(1-v)I}{N}$. The modified SEIRS model reads

$$\left\{\begin{array}{lcl} \frac{dS}{dt} & = & -\beta(1-v)^2\frac{SI}{N} + \gamma R \\ \frac{dE}{dt} & = & \beta(1-v)^2\frac{SI}{N} - kE \\ \frac{dI}{dt} & = & kE - \alpha I \\ \frac{dR}{dt} & = & \alpha I - \gamma R \end{array}\right. \tag{1}$$

It is noticeable that the proportion of isolated individuals v is the same for the susceptible and infectious compartments: I represents the number of pre-symptomatic (infectious people who have not developed onsets yet) and asymptomatic (infectious without onset) individuals, who cannot be differentiated from susceptible individuals, and thus equally affected by NPI. Individuals who present onsets or who have been tested are supposed to be definitively isolated and removed from the dynamics, thus belonging to the removed class R. To summarize, v represents the proportion of isolated individuals for whom the status is unknown, while the isolation of individuals who have been recognized as infectious is part of the removal process corresponding to the term αI (see section 2.4 for more details on α).

Now we consider effect of mitigation policies which depend on the number of infected individuals, i.e. we impose that the proportion of individuals $v(I)$ in state 1 depends on the intensity of the epidemic, i.e. the number of infected individuals I.

Since the dynamics of R can be deduced from the ones of S, E and I, the dynamics is governed by the system

$$\left\{\begin{array}{lcl} \frac{dS}{dt} & = & -\beta(1-v(I))^2\frac{SI}{N}+\gamma(N-S-E-I) \\ \frac{dE}{dt} & = & \beta(1-v(I))^2\frac{SI}{N}-kE \\ \frac{dI}{dt} & = & kE-\alpha I \end{array}\right. \tag{2}$$

The resulting model is a SEIRS model with a modified transmission rate that reflects the NPI intensity which changes with the number of infected individuals. However, the classical SEIRS models can only have one endemic equilibrium while the model with NPI can have several endemic equilibria and a different dynamics. The model obtained with constant v is similar to the one in [4].

Finally, we must address the issue of the large number of asymptomatic people for SARS-CoV-2. In our model, symptomatic and asymptomatic individuals have not been considered separately. Regarding to the model, they only differ on the time spent in the infectious compartment. Thus they are considered as belonging to a same infectious compartment, and an average value for the parameter α is estimated in order to represent such heterogeneity. A detailed justification and estimation of α is presented in section 2.4.

2.2. Endemic equilibria

$(N,0,0)$ is the Disease Free Equilibrium (DFE). Interior endemic equilibria (S^*,E^*,I^*) verify:

$$\left\{\begin{array}{l} \beta(1-v(I^*))^2\frac{S^*I^*}{N}=\gamma(N-S^*-E^*-I^*) \\ \beta(1-v(I^*))^2\frac{S^*I^*}{N}=kE^* \\ kE^*=\alpha I^* \end{array}\right. \tag{3}$$

The equilibrium susceptible population can be expressed in terms of the infected one:

$$S^*=N-\left(1+\frac{\alpha}{k}+\frac{\alpha}{\gamma}\right)I^* \tag{4}$$

The infected population I^* verifies the following expression:

$$\frac{\beta}{N}(1-v(I^*))^2\left(N-\left(1+\frac{\alpha}{k}+\frac{\alpha}{\gamma}\right)I^*\right)=\alpha \tag{5}$$

Let us define the function $\hat{v}$ such that for $I\geq 0$,

$$\hat{v}(I)=1-\frac{1}{\sqrt{\mathcal{R}_0-\frac{\beta}{N}\left(\frac{1}{\alpha}+\frac{1}{k}+\frac{1}{\gamma}\right)I}} \tag{6}$$

where $\mathcal{R}_0=\frac{\beta}{\alpha}$ is the basic reproduction rate of the SEIRS epidemic. We deduce from equation (5) that at endemic equilibria, the equality

$$v(I^*)=\hat{v}(I^*) \tag{7}$$

holds. For a given control function v associated to a given set of mitigation measures, the set of endemic equilibria can be determined by finding the solution of equation (7). In other words, each time that the graph of the chosen function v intersects the function $\hat{v}$, it corresponds to an endemic equilibrium, as it will be illustrated in the next section.

Function $\hat{v}$ is a monotonously decreasing function and intersects the abscesses axis at the classical endemic equilibrium $I_{EE} = \frac{\mathcal{R}_0 - 1}{\frac{\beta}{N}\left(\frac{1}{\alpha}+\frac{1}{k}+\frac{1}{\gamma}\right)}$, reached in absence of mitigation measures ($v = 0$). We also note that $\hat{v}(0) = 1 - \frac{1}{\sqrt{\mathcal{R}_0}}$. As shown in the appendix, the disease free equilibrium (DFE) is stable if and only if $v(0) > 1 - \frac{1}{\sqrt{\mathcal{R}_0}}$.

2.3. Stability analysis

We now study the dynamics of the SEIRS model by finding the stability of the equilibria (DFE and endemic equilibria). For the sake of simplicity, we assume that v is $\mathcal{C}^1$ around the equilibria. The Jacobian matrix for the SEIRS Model (2) reads:

$$J = \begin{pmatrix} -\frac{\beta}{N}(1-v(I))^2 I - \gamma & -\gamma & -\frac{\beta}{N}(1-v(I))^2 S - \gamma + 2\frac{\beta}{N}v'(I)(1-v(I))IS \\ \frac{\beta}{N}(1-v(I))^2 I & -k & \frac{\beta}{N}(1-v(I))^2 S - 2\frac{\beta}{N}v'(I)(1-v(I))IS \\ 0 & k & -\alpha \end{pmatrix} \tag{8}$$

2.3.1. Local stability of the DFE

For the DFE, $(N, 0, 0)$, the Jacobian reads

$$J_{DFE} = \begin{pmatrix} -\gamma & -\gamma & -\gamma - \beta(1-v(0))^2 \\ 0 & -k & \beta(1-v(0))^2 \\ 0 & k & -\alpha \end{pmatrix} \tag{9}$$

We are ensured to find one negative eigenvalues, $\lambda_1 = -\gamma < 0$. We consider the remaining minor matrix J_{MIN}:

$$J_{MIN} = \begin{pmatrix} -k & \beta(1-v(0))^2 \\ k & -\alpha \end{pmatrix} \tag{10}$$

We find that its trace, $Tr(J_{MIN}) = -k - \alpha$ is negative and that the determinant, $det(J_{MIN}) = k(\alpha - \beta(1-v(0))^2)$ can be positive or negative. It is positive when $v(0) > 1 - \frac{1}{\sqrt{\mathcal{R}_0}}$. Under these conditions, the DFE is stable and it is possible to generate an Allee effect.

2.3.2. Local stability for an endemic equilibrium

For any interior equilibrium (S^*, E^*, I^*), the Jacobian matrix simplifies by incorporating equilibrium expressions (3):

$$J^* = \begin{pmatrix} -\gamma - \frac{kE^*}{S^*} & -\gamma & -\gamma - \alpha + 2\frac{kv'(I^*)E^*}{(1-v(I^*))} \\ \frac{kE^*}{S^*} & -k & \alpha - 2\frac{kv'(I^*)E^*}{(1-v(I^*))} \\ 0 & k & -\alpha \end{pmatrix} \tag{11}$$

The characteristic equation reads as follows:

$$\lambda^3 + a_1\lambda^2 + a_2\lambda + a_3 = 0 \tag{12}$$

with:

$$a_1 = \left(\alpha + k + \gamma + \frac{kE^*}{S^*}\right) > 0 \tag{13}$$

$$a_2 = (\alpha + k + \gamma)\frac{kE^*}{S^*} + \gamma(k + \alpha) + 2\frac{k^2 v'(I^*)E^*}{(1 - v(I^*))} \tag{14}$$

$$a_3 = 2\frac{\gamma k^2 v'(I^*)E^*}{(1 - v(I^*))} + (\alpha\gamma + \gamma k + \alpha k)\frac{kE^*}{S^*} > 0 \tag{15}$$

The Routh-Hurwitz conditions $a_1 > 0$ and $a_3 > 0$ are always verified for a positive interior endemic equilibrium. If $v'(I^*) > 0$, it is easy to check that the last Routh-Hurwitz condition is also verified. Indeed, after simplification, $a_1 a_2 > a_3$ reads:

$$\begin{aligned}(\alpha^2 + k^2 + \gamma^2 + \alpha k + \alpha\gamma + k\gamma)\frac{kE^*}{S^*} + (\alpha + k + \gamma)\left(\frac{kE^*}{S^*}\right)^2 \\ + \gamma(k + \alpha)\left(\alpha + k + \gamma + \frac{kE^*}{S^*}\right) + 2k^2\left(\alpha + k + \frac{kE^*}{S^*}\right)\frac{v'(I^*)E^*}{1 - v(I^*)} > 0\end{aligned} \tag{16}$$

It is always verified for a positive endemic equilibrium when $v'(I^*) > 0$. In other words, if the level of protection increases with the number of infected individuals, the endemic equilibrium is stable. It is still true when $v'(I^*) < 0$ and $|v'(I^*)|$ is small. In other cases ($v'(I^*) < 0$ and $|v'(I^*)|$ is larger than a given threshold), the equilibrium is unstable.

As a consequence, the stability of endemic equilibria is independent of the stability of the DFE, and equilibria with the same stability can coexist.

2.4. Dynamics without protection measures: parameters estimation based on Covid-19

In the absence of confinement ($v = 0$), the dynamics follows the one of a classical SEIRS model, tending towards the endemic equilibrium with decreasing oscillations. Parameters of the model can be estimated from various medical and statistical reports about Covid-19.

Parameter k can be estimated around 0.2 day^{-1} since the average incubation time is 5.2 days [15].

Parameter α has to incorporate the heterogeneity of time spent in infectious compartment by symptomatic and asymptomatic individuals. Let us assume that a proportion f of those infectious individuals are asymptomatic and are removed from the infectious compartment after healing at a rate α_a, while a proportion $(1 - f)$ of individuals have severe symptoms or are detected early and are treated in hospital or quickly quarantined. They are removed at a rate $\alpha_s > \alpha_a$. It was found that infectiousness can occur from 2.3 days (95% CI, 0.8-3.0 days) before symptom onset, significantly declines 10 days after onset, with a peak at 0.7 days (95% CI, -0.2–2.0 days) before onset ([9]). Considering that,

acceptable values may be $\alpha_s = 1$ and $\alpha_a = 0.1$. In our model, we consider an average value for the parameter α that is given by

$$\alpha = (1 - f)\alpha_s + f\alpha_a \tag{17}$$

In [22], it is reported that on tests carried out in France, just under 50% of people who are tested positive are asymptomatic. The value of parameter α may vary between 0.1 and 1, with $\alpha = 5.5$ when $f = 0.5$. As a consequence, we set $\alpha = 0.5$ in this model.

$\mathcal{R}_0 = \frac{\beta}{\alpha}$ has been estimated between 2 and 6, with most probable values in the range 2-3 [10]. In our model, we set $\beta = 1.5$ in order to obtain $\mathcal{R}_0 = 3$.

Finally, there is a major uncertainty about parameter γ at the time being, since there are only a few hints about the duration of immunity, or even if the loss of immunity is possible or not. Few cases of re-infections have been observed, [20]. Accordingly, the γ parameter should be small. However, the appearance of new variants of the virus seems likely to cause re-infection with SARS-CoV-2 [6, 24].

Figure 1 compares several dynamics in the total absence of protective measures, scaled to a population of 100,000 individuals for different values of γ. It shows that considering different values for γ lead to the same qualitative dynamics. Despite the large range for γ, the amplitude of the first peak is similar, while the second one is shifted in time but has a similar amplitude (Figure 1a and 1c). Reinfection causes an infinite growth of the cumulative cases (Figure 1b).

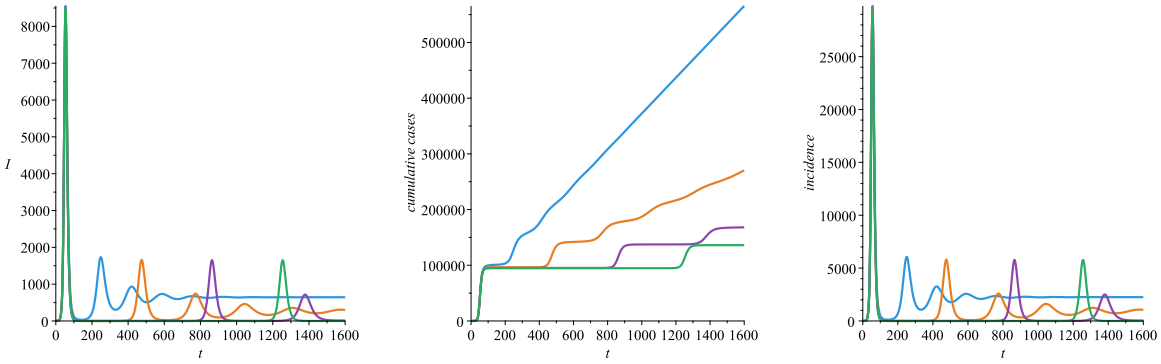

(a) Active cases (b) Cumulative cases (c) Incidence rate

Figure 1: Evolution of the epidemic in the absence of confinement $v = 0$, for $1/\gamma = 200$ (blue), 500 (orange), 1000 (purple) and 1500 (green): (a) active cases, (b) cumulative cases and (c) incidence rate (number of new cases per week), for a population of 100,000 individuals. The initial conditions is $(S(0) = N - 1, E(0) = 0, I(0) = 1)$. Parameters values are $\beta = 1.5$, $k = 0.2$, and $\alpha = 0.5$.

The incidence rate (number of new cases per week per 100,000 individuals) decreases with $1/\gamma$. However Figure 1c illustrates that if no control measures are taken, it remains high for a large range of values. With any value of $1/\gamma$ below approximately 2300 days, the incidence rate at the equilibrium is over 200. Even for higher values of $1/\gamma$, the dynamics still present large peaks over 200. Such a value is considered as high: in USA, CDC (Center

for Disease Control and Prevention) consider countries with an incidence rate of 25 cases per week as high risk countries [8], and in France, an alert threshold has been set at 250. Therefore it is necessary to define NPI strategies in order to achieve this, since the wide range for γ might be compatible with possible real values. We will now present several possible strategies to fight against the epidemic when it starts.

3. Presentation of various NPI strategies to fight the epidemic

Based on the mathematical analysis of the model, we consider four main classes of epidemic NPI strategies: a first one consisting in a constant control, a second one stabilizing the epidemic at a sufficiently low target endemic level, a third one aiming at the eradication of the epidemic. We also consider a fourth class which is a combination of strategies two and three. In order to compare the various strategies, all simulations shown from now on use the same set of epidemiological parameters: $\beta = 1.5$, $k = 0.2$, $\alpha = 0.5$, $N = 100{,}000$ and $\gamma = 1/200$.

3.1. Strategy 1: constant control

As shown on Figure 2, we compare four constant control strategies with different intensities. The two highest intensity strategies ($v = 0.8$: blue and $v = 0.5$: orange) have no endemic equilibria and a stable DFE (Figure 2(a)). They lead to the extinction of the epidemics (Figure 2(b)). The two others ($v = 0.3$: purple and $v = 0.2$: green) have a stable endemic equilibrium and an unstable DFE. The number of active cases I shows oscillations and stabilizes around the endemic equilibrium. The value at the equilibrium is lower for a more intense strategy. Peaks appear, corresponding to different waves of infection. The most intense strategy show lower peaks which are more distant in time. The number of cumulative cases keeps increasing as people gets reinfected, its value eventually become larger than the total population. The incidence rate, number of new cases I per 100,000 inhabitants per week is given by kE according to system 2. It is approximately obtained by scaling and shifting the curve of I.

With a NPI intensity v high enough, the curve of v remains above the one of $\hat{v}$ and the epidemics goes extinct: the number of active cases falls below 1 in around 100 days for $v = 0.5$ and around 20 days for $v = 0.8$.

3.2. Strategy 2: lower the endemic equilibrium (NPI intensity increasing with "I")

In order to obtain a unique endemic equilibrium, we choose a family of increasing monotonic maps $v(I)$ $v : I \mapsto v_0 I/(I + 100)$ for different values of $v_0 = 0.8, 0.5$ and 0.3 (see Figure 3). The intersection with the curve $\hat{v}$ defines an endemic equilibrium I^* which is locally asymptotically stable. The dynamics also present an unstable DFE. The value of I^* decreases with v_0: I^* is respectively around 400, 200 and 50 for $v_0 = 0.8, 0.5$ and 0.3. High values of v_0 lead to a rapid decrease of the epidemic, while a low value (purple curve) still allow large amplitude peaks, that may not be manageable by hospitals.

As expected, the cumulative number of cases decreases with the target endemic level. It seems to be a natural strategy, with the intensity of measures increasing with the level

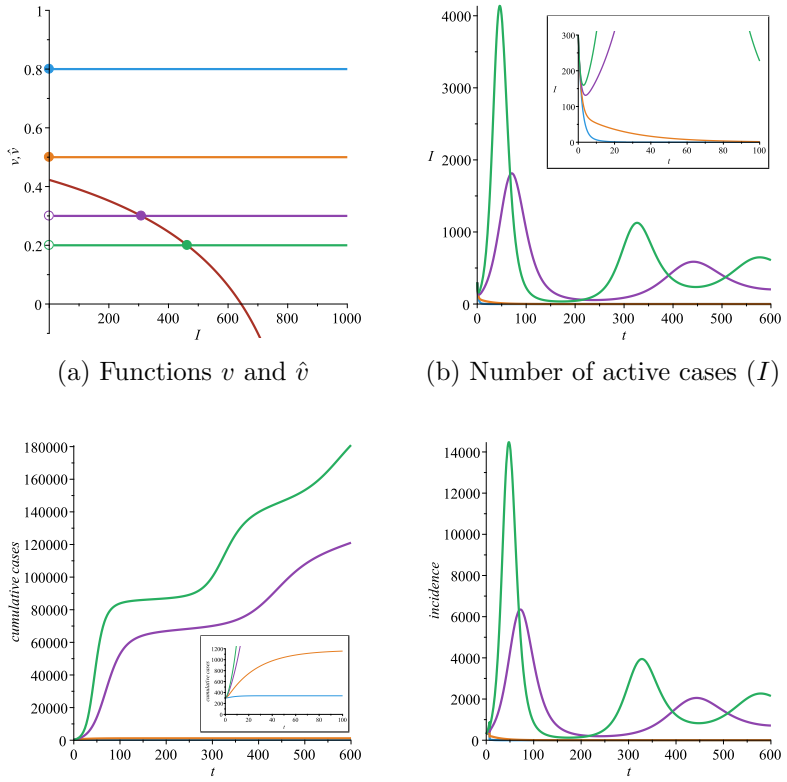

(a) Functions v and $\hat{v}$

(b) Number of active cases (I)

(c) Cumulative cases

(d) Incidence rate

Figure 2: Comparison of constant control strategies: $v = 0.8$ (blue), $v = 0.5$ (orange), $v = 0.3$ (purple), $v = 0.2$ (green), for a population of 100,000 individuals. Parameters values are $\beta = 1.5$, $k = 0.2$, $\alpha = 0.5$ and $\gamma = 1/200$. The initial condition is $(S(0) = N - 300, E(0) = 0, I(0) = 300)$. (a) comparison of functions v and $\hat{v}$, with stable (solid circles) and unstable (empty circles) equilibria. (b) evolution of the number of active cases I. An insert show the details of the region $0 < t < 100$. (c) Evolution of the number of cumulative cases. (d) Evolution of the incidence rate (number of new cases per 100,000 inhabitants per week).

of epidemics, since many governments choose to have a light level of social distancing at low level of incidence, and harder measures at higher levels. This strategy may turn useful to keep the epidemic low enough to prevent hospital congestion with a lower level of active cases. However it comes along with moderate intensity but never-ending measures as it is not possible to reach the extinction of the epidemics (Figure 3d).

3.3. Strategy 3: generating an Allee effect

An Allee effect can be generated by choosing a control function that stabilizes the DFE. Decreasing functions create a new unstable endemic equilibrium at a lower level. If a stable endemic equilibrium remains, he may have a reduced basin of attraction. As an illustration, we choose the following family of piecewise linear maps:

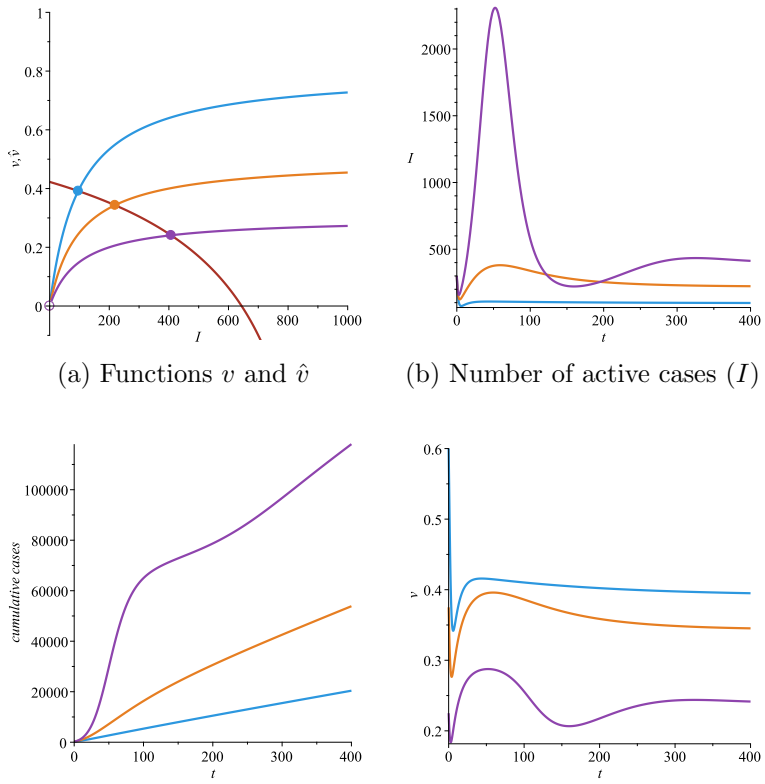

(a) Functions v and $\hat{v}$ (b) Number of active cases (I)

(c) Cumulative cases (d) NPI intensity $v(t)$

Figure 3: Comparison of strategies lowering the endemic equilibrium. Chosen functions are $v : I \mapsto v_0 I/(I + 100)$, with $v_0 = 0.8$ (blue), $v_0 = 0.5$ (orange) and $v_0 = 0.3$ (purple). Parameters values are $\beta = 1.5$, $k = 0.2$, $\alpha = 0.5$ and $\gamma = 1/200$. The initial condition is $(S(0) = N - 300, E(0) = 0, I(0) = 300)$. (a) comparison of functions v and $\hat{v}$, with stable endemic equilibria (solid circles), and an unstable DFE (empty circle). (b) evolution of the number of active cases I. (c) Evolution of the number of cumulative cases. (d) NPI intensity $v(t)$.

$$v : I \mapsto \begin{cases} v_0 \left(1 - \frac{I}{I_{max}}\right) & \text{if } 0 \leq I < I_{max} \\ 0 & \text{if } I_{max} \leq I \end{cases} \tag{18}$$

with $v_0 = 0.8$ and $I_{max} = 400$ (blue), 100 (orange) and 900 (purple) (see Figure 4a). Blue and orange maps create a lower unstable endemic equilibrium and have another higher stable endemic equilibrium, while the purple curve stays above $\hat{v}$ and have no associated endemic equilibrium. The dynamics is represented for two sets of initial conditions: $S_0 = N - 300$, $E_0 = 0$, $I_0 = 300$, and $S_0 = 60{,}000$, $E_0 = 1000$, $I_0 = 200$.

An "Allee" type effect is observed: depending on the initial conditions, the epidemics may disappear or tend towards an high endemic equilibrium. The basins of attraction of the endemic equilibria for the different measures are represented in their respective colors in Figure 4d. Stronger measures lead to smaller basin of attraction for the endemic

equilibrium: the one of the blue measure is included in the one of the orange measure, and the risk to be trapped around the endemic equilibrium is lower, thus it comes at a cost of longer and more intense NPI (Figure 4e). Indeed, the second initial condition is in the orange basin of attraction of the endemic equilibrium, while not in the blue one. The intensity of measures is also higher than the ones for strategy 2. It is remarkable that initial conditions with few infected individuals (small I and E) are in the basin of attraction of the DFE.

Such strategies still present the risk of peaks, even if the epidemic eventually vanishes. Orange curves present peaks for both initial conditions: with the first one, the epidemics disappear after a peak (dark orange), and with the second one (light orange curves), the system tends towards an endemic equilibrium (Figure 4b), leading to an always increasing epidemic (Figure 4c). The blue measure, with a higher unstable endemic equilibrium, only has a peak for the second initial condition. Figure 4d shows surfaces in the phase portrait delimiting the domain in which initial conditions lead to a peak (domain under the surface) from the domain in which they prevent a peak (domain above the surface an containing the line $I = E = 0$), a peak being defined here by the fact that the number of infected individuals I grows above I_0. It is to be noted that with this definition, it is not possible to distinguish high amplitude peaks (dark orange curve) from small amplitude peaks (light orange curve). More intense NPI lead to larger domains without peaks, though there is little difference between the surfaces.

Furthermore a "stop-and-go" effect can be observed for the light blue curve with two different periods of lockdown of very high intensity measures (around 0.7). The dynamic of the epidemic peak is very strong and explains the two confinement events separated by a period of absence of confinement. Indeed, when a high epidemic peak occurs, a first phase of confinement is observed. Thereafter, the peak descends until it returns below the threshold of the Allee effect, which causes the eradication of the epidemic thanks to the second phase of confinement.

Such a strategy may be less natural since it means higher intensity measures when I is low than when I is high. However the intensity is still lower than in strategy 1, and it can provoke the extinction of the epidemics, what cannot be achieved with strategy 2. A threshold of $I = 1$ is reached in around 40 days for the blue curve with the first initial condition. On the temporal level, the intensity of measures first increases as the number of cases decrease before reaching a threshold and stays high until the epidemics has been eradicated (we considered here that it happens when reaching the threshold $I = 1$). It should be noted that the number of cumulative cases in the case of the "Allee" effect is a bit higher but in the same order than in the case of confinement at a constant level of 0.8 (714 instead of 340 for the blue measure). Finally, the purple strategy also causes the eradication of the epidemic but without creating an unstable endemic equilibrium. In this case, the DFE is always stable because the $v(I)$ curve is always above the $\hat{v}(I)$ curve. This strategy makes it possible to bring about the disappearance of the epidemic in about 30 days with a single phase of confinement.

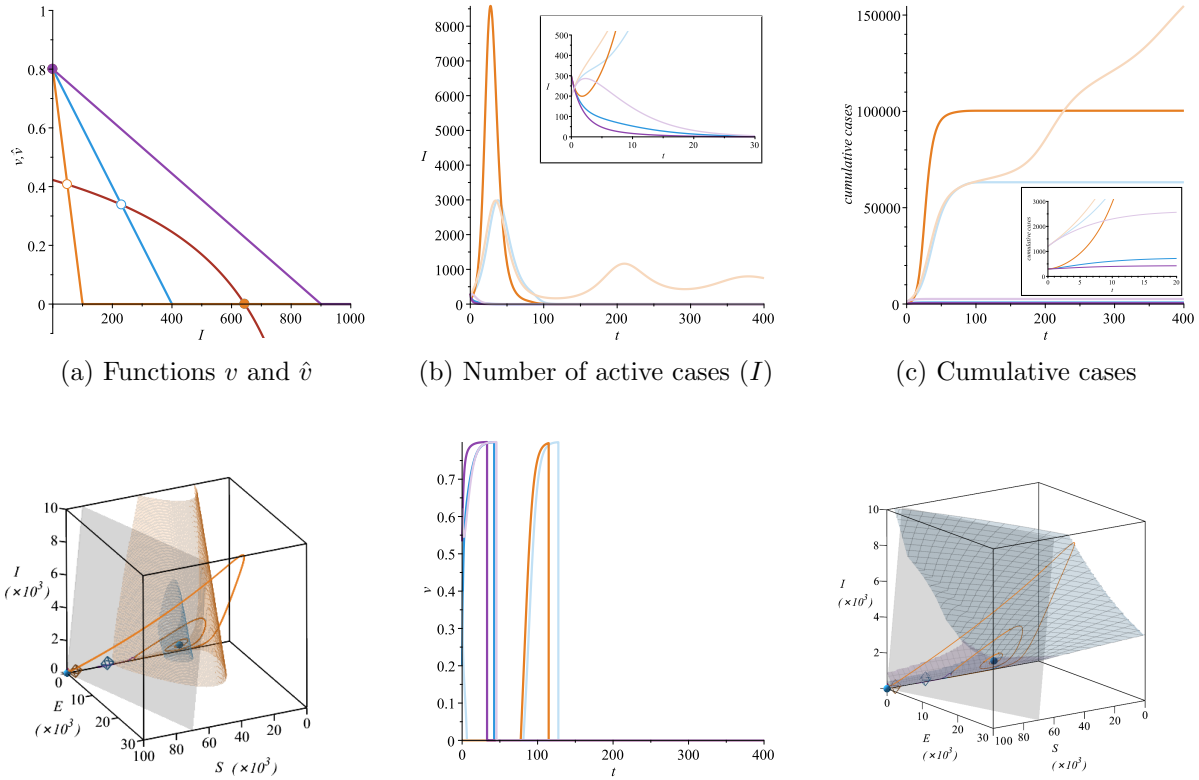

(a) Functions v and $\hat{v}$ (b) Number of active cases (I) (c) Cumulative cases

(d) Phase portrait (e) NPI intensity $v(t)$ (f) Peak/No peak domains

Figure 4: Comparison of control strategies which creates an Allee effect. Chosen functions are piecewise linear maps, decreasing from 0.8 to 0 from $I = 0$ to $I = I_{max}$ and equal to 0 elsewhere, with $I_{max} = 400$ (blue), $I_{max} = 100$ (orange) and $I_{max} = 900$ (purple). Parameters values are $\beta = 1.5$, $k = 0.2$, $\alpha = 0.5$ and $\gamma = 1/200$, for a population of 100,000 individuals. The initial conditions are $(S(0) = N - 300, E(0) = 0, I(0) = 300)$ (dark tones) and $S_0 = 60{,}000$, $E_0 = 1000$, $I_0 = 200$ (light tones). (a) comparison of functions v and $\hat{v}$, with a stable (solid circle) DFE and unstable (empty circles) endemic equilibria. (b) evolution of the number of active cases I. (c) Evolution of the number of cumulative cases. (d) Phase portrait. Stable equilibria are represented by a solid sphere, and unstable equilibria by a diamond. Their color correspond to the one of the respective map v. Colored surfaces indicate the basin of attractions of the stable endemic equilibrium, for $I_{max} = 400$ (blue), $I_{max} = 100$ (orange) and $I_{max} = 900$ (purple). The grey plane delimits the volume of possible initial conditions. (e) NPI intensity $v(t)$. (f) Frontier between the domains for which initial conditions lead/don't lead to a peak.

3.4. Strategy 4: combining an Allee effect and lowering the endemic equilibrium

We choose a family of simple piecewise linear functions to illustrate such combination. They first decrease in order to generate an Allee effect, then increase in order to lower the endemic equilibrium. Such maps are represented in Figure 5a and read:

$$v : I \mapsto \begin{cases} v_0 \left(1 - \frac{I}{I_1}\right) & \text{if } 0 \leq I < I_1 \\ 0 & \text{if } I_1 \leq I < I_2 \\ v_0 \left(\frac{I - I_2}{I_3 - I_2}\right) & \text{if } I_2 \leq I < I_3 \\ v_0 & \text{if } I_2 \leq I \end{cases} \tag{19}$$

Each of them generate a stable DFE, a low unstable endemic equilibrium, and a higher endemic equilibrium which is lower than the endemic equilibrium without NPI.

With an initial condition corresponding to a low infectious ($S_0 = N - 300$, $E_0 = 0, I_0 = 300$, dark colors in Figure 5b), the dynamics is the same than for the Allee effect, leading to the extinction of the epidemics. The second initial condition (($S_0 = 25{,}000$,$E_0 = 10{,}000, I_0 = 600$ light colors) corresponds to an already well installed epidemic lead to an endemic equilibrium for the orange and blue measures, while the purple one still lead to the extinction of the epidemics. However, even if it is located in the basin of attraction of the DFE for the purple strategy (Figure 5d) it generates an epidemic peak (Figure 5b).

The basin of attraction of the endemic equilibrium occupies the left part of the space in Figure 5d. It has a very different shape than the one for strategy 3 (Figure 4d) and encompasses a larger part of the phase space. The basin of attraction of the DFE occupies the right part of the space and a thin domain around the line $I = E = 0$, such that it includes initial conditions with a small number of infected individuals. Figure 5f shows the limit between the domain with peaks (lower space) from the one without peaks (upper domain). The domain without peaks is larger than for strategy 3 (Figure 4f).

Such a strategy has the advantage to lead to extinction of the epidemics as in strategy 3 if the initial condition is in the basin attraction of the DFE (Figure 5d), and avoid large peaks if measures are taken too late or if the level of the epidemics has been underevaluated. The basin of attraction of the endemic equilibrium is much larger than in strategy 3. It can be seen as a drawback, since more initial conditions will lead to an endemics equilibrium, or a benefit, since such initial conditions would lead to a large peak with strategy 3, while strategy 4 limits the amplitude of the peak.

4. Discussion

In this work, we have shown that we can control an epidemic when it starts by imposing a level of NPI which depends on the number of infected persons each day. To summarize our results, we considered an early epidemic at the scale of 100,000 inhabitants. We have shown that in the absence of protective measures, a peak of infected cases of the order of 9,000 people will occur and last for around 100 days. We then proposed several strategies to control the epidemic. The first class of strategies (blue) corresponds to a constant level of protection. The objective of the second class (orange) is to keep the epidemic at a fairly

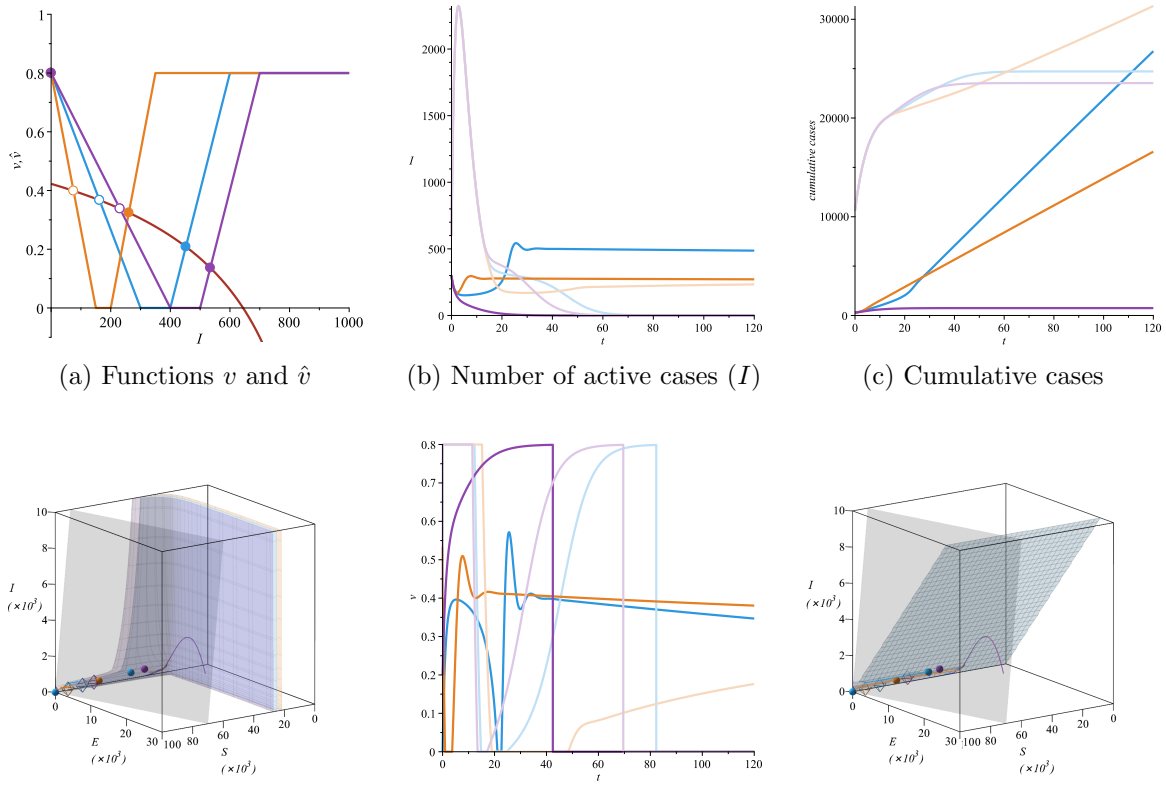

(a) Functions v and $\hat{v}$ (b) Number of active cases (I) (c) Cumulative cases

(d) Phase portrait (e) NPI intensity $v(t)$ (f) Peak/No peak domains

Figure 5: Comparison of strategies combining an Allee effect and a low endemic equilibrium. Parameters values are $\beta = 1.5$, $k = 0.2$, $\alpha = 0.5$ and $\gamma = 1/200$, for a population of 100,000 individuals. The initial conditions are $(S(0) = N - 300, E(0) = 0, I(0) = 300)$ (dark tones) and $(S(0) = 25{,}000, E(0) = 10{,}000, I(0) = 600)$ (light tones). (a) comparison of functions v and $\hat{v}$, with stable (solid circles) and unstable (empty circles) equilibria. (b) evolution of the number of active cases I. (c) Evolution of the number of cumulative cases. (d) Phase portrait. Stable equilibria are represented by a solid sphere, and unstable equilibria by a diamond. Their color correspond to the one of the respective map v. Colored surfaces indicate the basin of attractions of the stable endemic equilibrium. The grey plane delimits the volume of possible initial conditions. (e) NPI intensity $v(t)$. (f) Frontier between the domains for which initial conditions lead/don't lead to a peak.

low endemic level. The third (purple) and fourth (green) ones cause the epidemic to end. Additionally, for the fourth strategy, a lower endemic is created in order to avoid large peaks if the epidemics cannot be driven to extinction. The four strategies are compared on Figure 6. Strategies 2 and 4 have been chosen such that they have the same endemic equilibrium (Figure 6a).

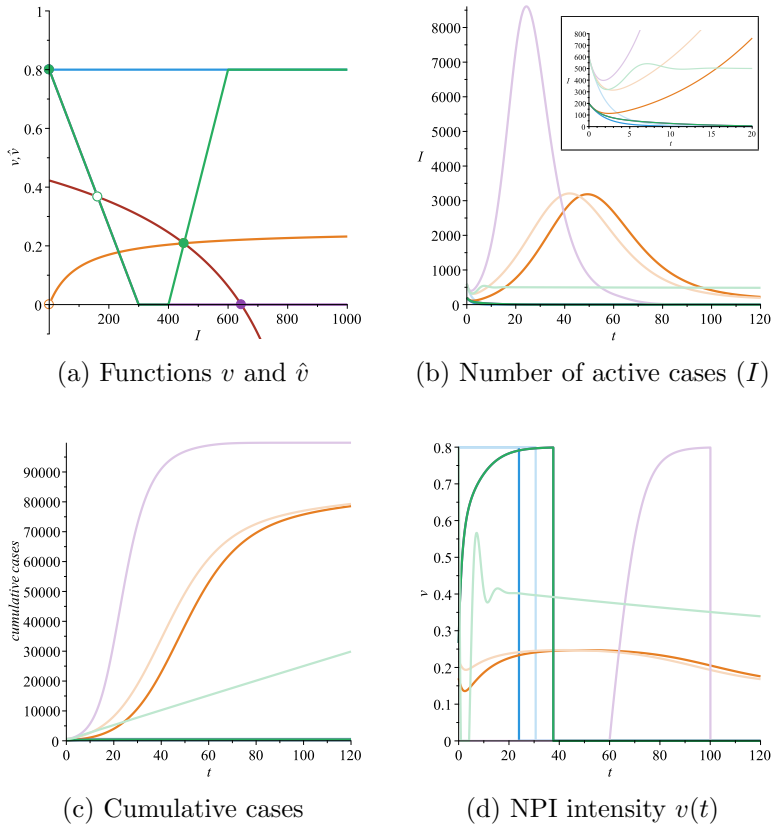

(a) Functions v and $\hat{v}$

(b) Number of active cases (I)

(c) Cumulative cases

(d) NPI intensity $v(t)$

Figure 6: Comparison of the different NPI strategies: constant control (blue), lower endemic equilibrium (orange), Allee effect (purple) and mix strategy (gree). Parameters values are $\beta = 1.5$, $k = 0.2$, $\alpha = 0.5$ and $\gamma = 1/200$, for a population of 100,000 individuals. The initial conditions are $(S(0) = N - 300, E(0) = 0, I(0) = 300)$ (dark tones) and $(S(0) = 60{,}000, E(0) = 1000, I(0) = 200)$ (light tones). (a) comparison of functions v and $\hat{v}$, with stable (solid circles) and unstable (empty circles) equilibria. (b) evolution of the number of active cases I. (c) Evolution of the number of cumulative cases. (d) NPI intensity $v(t)$.

Strategies 1, 3 and 4 make the DFE stable. However, extinction of the epidemics may depend on initial conditions: it is always achieved for strategy 1 (blue), but may fail for strategies 3 (purple) and 4 (green). Furthermore, strategy 3 (purple) still presents a risk of a peak (Figure 6b) followed by a second phase of intense NPI such as a lockdown (Figure 6d), even if the epidemic eventually vanishes.

Strategy 1 (blue, constant and very high confinement at 0.8) has the shortest total NPI duration but may be difficult to implement from the start. In practice, it may be very difficult to impose NPI at such a very high level (0.8), or at least it may require some time

to be achieved. Strategies 3 and 4 have the advantage to propose NPI with a gradually increasing intensity in time that reach the maximum value at the end of the epidemic. For the first initial condition, strategies 3 (purple) and 4 (green) can be seen as equivalent to strategy 1 (blue), (the dark green curve overlaps the dark purple curve on Figure 6d) in term of duration before the extinction of the epidemic. It takes 28 days to end the epidemic for strategy 1 and 38 for strategies 3 and 4, but the latter have the advantage of installing the confinement gradually over a period of about three weeks from 0.4 to 0.8, with a number of cumulative cases a bit higher.

However, such strategies may seem counter-intuitive in the sense that it is necessary to strengthen the NPI intensity as the number of infected decreases in order to achieve the eradication of the epidemic in some time frame. Indeed it is the opposite in most countries. For example, in France, two lockdowns have been established and a third one is being considered. For each lockdown, its intensity has been reduced when the epidemic peak has diminished sufficiently so as not to saturate the hospitals but without maintaining it long enough at a high level to bring about the eradication of the epidemic. These successive confinements have generated astronomical infectious and economic costs. Epidemic waves seem to endlessly followed each other unless a vaccination policy can achieve collective immunity.

Strategies 2 and 4 create a lower endemic equilibrium that helps reducing the amplitude of peaks: orange and green curves present a much lower peak than the purple strategy (6b). In strategy 2 (orange), we use an increasing monotonic protection function which allows to create a unique and stable endemic equilibrium at a sufficiently low target level. This strategy helps stabilizing the epidemic at this desired constant level but lead to an endless NPI that may be economically and socially costly. This strategy corresponds more or less to the current NPI in many countries, such as masks, social distancing, closure of restaurants and public places, teleworking at a rather constant level. When the health situation worsens, the level of measures is reinforced for some weeks in order to return to a lower level of virus circulation, resulting in successive epidemic waves. Such phenomenon also appears for strategy 4 (green) for unfavourable initial conditions, that is when the epidemics is handled too late.

The mix strategy 4 combines the benefits of strategies 2 and 3: extinction of the epidemics with progressive NPI for favourable initial conditions (dark green curve in Figure 6b), lower peak when for unfavourable ones (light green curve), associated to lower intensity NPI (Figure 6d). However, some initial conditions which lead to the extinction of the epidemic for strategy 3 may only lead to a lower endemic equilibrium with strategy 4 (light purple and light green curves in Figure 6).

5. Conclusion and perspectives

In this paper, we have shown that NPI strategies may be divided into three main classes. We have highlighted the benefits and drawbacks of those classes, such as ability to put an end to the epidemics in the context of possible reinfection, duration of the epidemics, amplitude of the peaks and feasibility of the considered measures. Extinction

of the epidemics may be reached at the cost of NPI that may be too intense to be practically usable (strategy 1), or at the risk of a high epidemic peak (strategy 3) or being stuck at a lower endemic equilibrium (strategy 4). Finally, if only low intensity NPI may be used, strategy 2 may be applied, but at the cost of a never ending epidemic. Classes of strategies which bring about the disappearance of the epidemic once and for all may nevertheless seem to be the best option, as long as it is possible to impose high intensity NPI. The great advantage of such strategies is that, with an adequate choice of the $v(I)$ function, it is possible to eradicate the epidemic in a relatively short time of about 30 up to 50 days with rather limited cumulative infectious cases.

In our opinion, these epidemic control methods could be used locally for medium-sized cities where the epidemic is restarting. The application of these classes of strategies would require the use of a significant number of tests allowing a good estimation of the numbers of infected people at the time when the control must be implemented. It requires to properly position the various endemic equilibria created by the epidemic control function. It may also be applicable to any other disease that can be modelled with a SEIRS model.

As a perspective, we could study a network of several cities connected by the movement of individuals from one city to another by rail or by plane. It would be interesting to study the coupling of epidemic management methods depending on the number of infected people in the different cities. We refer to [3] and [2], for disease spread in meta-populations.

We are inclined to think that our conclusions obtain through a theoretical approach on the effectiveness of the various strategies can be useful for practical case studies, as density dependent protection strategies could be used to target a sufficiently low level of endemicity or find a strategy to put an end to the epidemic while considering constraints such as social cost or hospitals capacity.

References

[1] David Adam. Modelling the pandemic the simulations driving the world's response to covid-19. *Nature*, 580(7803):316–318, 2020.

[2] Julien Arino and P Van den Driessche. Disease spread in metapopulations. *Fields Institute Communications*, 48(1):1–13, 2006.

[3] Julien Arino and Pauline Van Den Driessche. The basic reproduction number in a multi-city compartmental epidemic model. In *Positive Systems*, pages 135–142. Springer, 2003.

[4] Pierre Auger and Ali Moussaoui. On the threshold of release of confinement in an epidemic seir model taking into account the protective effect of mask. *Bulletin of mathematical biology*, 83(4):1–18, 2021.

[5] Nicolas Bacaër. Un modèle mathématique des débuts de l'épidémie de coronavirus en france. *Mathematical Modelling of Natural Phenomena*, 15:29, 2020.

[6] Ewen Callaway. Fast-spreading covid variant can elude immune responses. *Nature*, 589(7843):500–501, 2021.

[7] Centers for Disease Control. `https://www.cdc.gov/nhsn/covid19/report-patient-impact.html`, 2021.

[8] Centers for Disease Control. `https://www.cdc.gov/coronavirus/2019-ncov/travelers/how-level-is-determined.html`, 2021.

[9] Xi He, Eric HY Lau, Peng Wu, Xilong Deng, Jian Wang, Xinxin Hao, Yiu Chung Lau, Jessica Y Wong, Yujuan Guan, Xinghua Tan, et al. Temporal dynamics in viral shedding and transmissibility of covid-19. *Nature medicine*, 26(5):672–675, 2020.

[10] Joe Hilton and Matt J Keeling. Estimation of country-level basic reproductive ratios for novel coronavirus (sars-cov-2/covid-19) using synthetic contact matrices. *PLoS computational biology*, 16(7):e1008031, 2020.

[11] Jeremy Howard, Austin Huang, Zhiyuan Li, Zeynep Tufekci, Vladimir Zdimal, Helene-Mari van der Westhuizen, Arne von Delft, Amy Price, Lex Fridman, Lei-Han Tang, et al. An evidence review of face masks against covid-19. *Proceedings of the National Academy of Sciences*, 118(4), 2021.

[12] Stephen M Kissler, Christine Tedijanto, Edward Goldstein, Yonatan H Grad, and Marc Lipsitch. Projecting the transmission dynamics of sars-cov-2 through the post-pandemic period. *Science*, 368(6493):860–868, 2020.

[13] Adam J Kucharski, Petra Klepac, Andrew JK Conlan, Stephen M Kissler, Maria L Tang, Hannah Fry, Julia R Gog, W John Edmunds, Jon C Emery, Graham Medley, et al. Effectiveness of isolation, testing, contact tracing, and physical distancing on reducing transmission of sars-cov-2 in different settings: a mathematical modelling study. *The Lancet Infectious Diseases*, 20(10):1151–1160, 2020.

[14] Toshikazu Kuniya. Prediction of the epidemic peak of coronavirus disease in japan, 2020. *Journal of clinical medicine*, 9(3):789, 2020.

[15] Stephen A Lauer, Kyra H Grantz, Qifang Bi, Forrest K Jones, Qulu Zheng, Hannah R Meredith, Andrew S Azman, Nicholas G Reich, and Justin Lessler. The incubation period of coronavirus disease 2019 (covid-19) from publicly reported confirmed cases: estimation and application. *Annals of internal medicine*, 172(9):577–582, 2020.

[16] Yang Liu, Zhonglei Gu, Shang Xia, Benyun Shi, Xiao-Nong Zhou, Yong Shi, and Jiming Liu. What are the underlying transmission patterns of covid-19 outbreak? an age-specific social contact characterization. *EClinicalMedicine*, 22:100354, 2020.

[17] Zhihua Liu, Pierre Magal, Ousmane Seydi, and Glenn Webb. Understanding unreported cases in the covid-19 epidemic outbreak in wuhan, china, and the importance of major public health interventions. *Biology*, 9(3):50, 2020.

[18] Ali Moussaoui and Pierre Auger. Prediction of confinement effects on the number of covid-19 outbreak in algeria. *Mathematical Modelling of Natural Phenomena*, 15:37, 2020.

[19] Ali Moussaoui and El Hadi Zerga. Transmission dynamics of covid-19 in algeria: The impact of physical distancing and face masks. *AIMS Public Health*, 7(4):816, 2020.

[20] Miyo Ota. Will we see protection or reinfection in covid-19? *Nature Reviews Immunology*, 20(6):351–351, 2020.

[21] T Alex Perkins, Valerie A Paz-Soldan, Steven T Stoddard, Amy C Morrison, Brett M Forshey, Kanya C Long, Eric S Halsey, Tadeusz J Kochel, John P Elder, Uriel Kitron, et al. Calling in sick: impacts of fever on intra-urban human mobility. *Proceedings of the Royal Society B: Biological Sciences*, 283(1834):20160390, 2016.

[22] Santé Publique France. `https://www.santepubliquefrance.fr/dossiers/coronavirus-covid-19/coronavirus-chiffres-cles-et-evolution-de-\la-covid-19-en-france-et-dans-le-monde/articles/covid-19-tableau-de-bord\-de-l-epidemie-en-chiffres`, 2021.

[23] Haoxuan Sun, Yumou Qiu, Han Yan, Yaxuan Huang, Yuru Zhu, and Song Xi Chen. Tracking and predicting covid-19 epidemic in china mainland. *medRxiv*, 2020.

[24] Richard L Tillett, Joel R Sevinsky, Paul D Hartley, Heather Kerwin, Natalie Crawford, Andrew Gorzalski, Chris Laverdure, Subhash C Verma, Cyprian C Rossetto, David Jackson, et al. Genomic evidence for reinfection with sars-cov-2: a case study. *The Lancet Infectious Diseases*, 21(1):52–58, 2021.

[25] Ashleigh R Tuite, David N Fisman, and Amy L Greer. Mathematical modelling of covid-19 transmission and mitigation strategies in the population of ontario, canada. *Cmaj*, 192(19):E497–E505, 2020.

[26] Shang Xia, Jiming Liu, and William Cheung. Identifying the relative priorities of subpopulations for containing infectious disease spread. *PloS one*, 8(6):e65271, 2013.